ELSEVIER

Catalysis Today 31 (1996) 145–161

CATALYSIS TODAY

Ring-shift isomerization of *sym*-octahydrophenanthrene into *sym*-octahydroanthracene. Effects of zeolite catalysts and equilibrium compositions

Wei-Chuan Lai [a], Chunshan Song [a,*], Adri van Duin [b], Jan W. de Leeuw [c]

[a] *Fuel Science Program, 209 Academic Projects Building, The Pennsylvania State University, University Park, PA 16802, USA*
[b] *Laboratory for Organic Chemistry and Catalysis, Delft University and Technology, 2628 BL Delft, The Netherlands*
[c] *Division of Marine Biogeochemistry, Netherlands Institute for Sea Research (NIOZ), P.O. Box 59, 1790 AB Den Burg, The Netherlands*

Abstract

The effects of zeolite catalysts and reaction conditions on the ring-shift isomerization of *sym*-OHP into *sym*-OHA were studied through experiments at 200–300°C under an initial pressure of 0.79 MPa N_2 or H_2. Eight catalysts were examined, including three hydrogen mordenites, two noble metal loaded mordenites, and three Y-zeolites. Among the three mordenites, the catalyst with lower acidity (HML8) displayed the best selectivity to *sym*-OHA but the lowest activity. Among the three Y-zeolites, best selectivity to *sym*-OHA was achieved with NiHY, which has lower acidity and lower content of stronger acid sites. The activity for *sym*-OHP conversion is: Pd/HM30A > Pt/HM30A > HY ≈ LaHY > HM20A > HM30A > HML8 > NiHY. The selectivity to *sym*-OHA decreases almost linearly with increasing conversion beyond the pseudo-equilibrium stage (about 50% conversion). The desirable condition over HML8 is 250°C for 0.5 h. The other catalysts with higher acidity (HM20A, HM30A, and HY) are promising catalysts at 200°C. Molecular mechanics calculations were performed to establish the upper limit of the catalytic conversion. The calculations and experimental results indicate that reaction temperature has a moderate effect on the equilibrium yield of *sym*-OHA, whose formation is favored at lower temperature. However, the experimentally determined equilibrium ratios of *sym*-OHA to *sym*-OHP (close to 1.3) are lower than the calculated values (2–2.6). The occurrence of simultaneous side reactions probably contributes to the shift of the equilibrium state of *sym*-OHA and *sym*-OHP.

Keywords: Zeolite; Catalyst; Isomerization; Octahydrophenanthrene; Octahydroanthracene; Molecular mechanics

1. Introduction

Phenanthrene and its derivatives are abundant in coal-derived liquids from coal carbonization, pyrolysis, and liquefaction; however, they are used in industries only to a very limited extent [1,2]. On the other hand, their isomers, anthracene and its derivatives such as *sym*-octahydroanthracene (*sym*-OHA), are more useful materials for industrial applications. Anthracene and its derivatives may be used as the starting materials for the manufacturing of dyestuffs, anthraquinone (an effective pulping accelerator), and pyromellitic dianhydride (PMDA, the monomer for polyimides such as Du Pont's Kapton) [1]. Thus, it is desirable to convert

* Corresponding author. Fax. (+1-814) 8653075, e-mail csong@psu.edu.

0920-5861/96/$32.00
PII S0920-5861(96)00032-6

sym-OHP *sym*-OHA

Scheme 1. Ring-shift isomerization of *sym*-OHP into *sym*-OHA.

phenanthrene derivatives to anthracene derivatives.

There has been much research on the catalytic hydroprocessing of phenanthrene and anthracene under high H_2 pressures at temperatures generally in excess of 350°C [3–11]. This work concerns the selective isomerization of partially hydrogenated phenanthrene (*sym*-OHP) and anthracene (*sym*-OHA). A well-known isomerization of hydroaromatic compounds is ring-contraction, such as the conversion of tetralin to 1-methylindane, and this type of isomerization has also been reported for *sym*-OHP [12]. However, information is still limited about the ring-shift isomerization of phenanthrene derivatives into anthracene derivatives [7]. It has been shown in our earlier exploratory work [13,14] that some chemically modified mordenites and Y-zeolites may selectively promote the transformation of *sym*-octahydrophenanthrene (*sym*-OHP) into *sym*-OHA, as shown in Scheme 1, at lower temperatures. Subsequently, Cook and Colgrove [15] reported the acid catalyzed isomerization of phenanthrene, anthracene, and *sym*-OHA under FCC conditions (482°C).

The objectives of this work are to clarify the effects of reaction conditions and catalyst properties on the catalytic isomerization of *sym*-OHP into *sym*-OHA and to establish the pseudo-equilibrium compositions. We wish to establish activity and selectivity and equilibrium compositional data that could lead an inexpensive way of making anthracene derivatives from phenanthrene derivatives. In order to find the theoretical equilibrium compositions of *sym*-OHP and *sym*-OHA, and to establish the upper limit of the catalytic conversion, molecular mechanics calculations were performed at the Delft University of Technology using the MM3 program and force field described by Allinger [16].

2. Experimental

2.1. Reactants and catalysts

The *sym*-OHA and *sym*-OHP chemicals were obtained from Aldrich Chemical Company and TCI America, respectively, and were used as received. Their purities were analyzed using gas chromatography (GC) and gas chromatography–mass spectrometry (GC-MS). The eight catalysts used in the catalytic isomerization reactions included: three hydrogen mordenites (HML8, HM20A, and HM30A), two noble metal loaded mordenites (Pt/HM30A and Pd/HM30A), a hydrogen Y zeolite (HY), and two metal ion-exchanged Y zeolites (LaHY and NiHY). The three H-mordenites (HML8, HM20A, and HM30A) with different molar ratios of SiO_2 to Al_2O_3 (17, 21, and 38, respectively), were prepared by heat treatment of three commercial ammonium mordenite samples [17]. Pt/HM30A and Pd/HM30A were prepared by incipient wetness impregnation method; i.e. the salt of platinum and palladium were dispersed into the mordenites by incipient wetness impregnation of corresponding aqueous H_2PtCl_6 or H_2PdCl_4 dissolved in hydrochloric acid. The noble metal loading on the support was kept at 6 wt%. The metal-loaded catalysts were calcined in air at 450°C for 2 h after being dried in a vacuum oven. The three Y zeolites (HY, LaHY, and NiHY) were prepared according to the procedures described elsewhere [18]. More details of the preparation and properties of the catalysts are described elsewhere [14,19].

2.2. Acidic properties by TGA and DSC

The acidity of catalysts were characterized by the temperature-programmed desorption of a base using thermogravimetric analysis (TGA) in combination with differential scanning calorimetry (DSC). *n*-Butylamine (*n*-BA) was chosen as the base for adsorption–desorption study; it was obtained from Aldrich Chemical Company and was used as received with a

purity of 99 + %. Prior to adsorption, the previously calcined catalysts were further thermally pre-treated under vacuum to remove moisture. The adsorption was performed by flowing *n*-BA vapor (saturated in dry N_2) through the catalyst at room temperature for 1 hour; N_2 with a flow rate of about 100 cm^3/min was used as a carrier gas. The base-saturated catalyst was then analyzed by TGA and DSC.

The desorption experiments were carried out with base-saturated catalyst contained in an uncovered alumina cell using a Mettler TG50 thermogravimetric balance. Samples of about 10 mg were used in each measurement and a purge gas (N_2) flow of 200 cm^3/min at room temperature was used. Before the thermal analysis was started, the base-saturated sample was kept at 30°C for 30 min with purge flow to remove any weakly adsorbed moisture, which might have occurred during the sample transfer process in air. The desorption temperature was programmed from 30 to 600°C at a heating rate of 10°C/min, and the decrease in weight with increasing temperature was monitored. TGA and DTG (differential thermogravimetry) data were then obtained. The desorption was also carried out in a high-pressure differential scanning calorimeter using Mettler Model DSC 27HP. About 7.5 mg of each of the catalysts was placed in an uncovered standard aluminum cell (40 μl), and was heated from 30 to 600°C at a rate of 10°C/min with an initial isothermal time of 30 min. The system was continuously purged with 100 cm^3/min of N_2.

2.3. Reaction procedure and product analysis

Catalytic isomerization reactions were mainly carried out in 28-ml horizontal type stainless steel tubing bomb reactors at 200–300°C for a heating period of 0.15–22 h under an initial pressure of 0.79 MPa ultra high purity (UHP; 99.999%) N_2 or H_2. A leak-tested reactor was charged with 0.6 mmol of *sym*-OHP or *sym*-OHA (0.112 g), 1 ml of 1,3,5-trimethylbenzene solvent, and 0.2 g of catalyst. The sample was deoxygenated through repetitive (6 times) pressurization to 6.9 MPa with UHP N_2 or H_2 and purging. The reactor was pressurized to the desired starting pressure of 0.79 MPa with N_2 or H_2 before being immersed into a fluidized sand bath which has been preheated to the desired reaction temperature, and agitated vertically at 240 cycles/min. The experiment was ended after the desired reaction time by removing the reactor from the fluidized sand bath and immediately quenching in a cold water bath. After the reaction, the gaseous products were collected in a gas bag, and the liquid products were recovered by washing with acetone. A non-catalytic run was carried out in the same 28-ml stainless steel tubing bomb reactor at 300°C for 1 h under an initial pressure of 0.79 MPa UHP N_2. The blank run showed no sign of ring-shift isomerization reaction in the stainless steel reactor at 300°C.

Some catalytic isomerization reactions were carried out in hermetically sealed aluminum cells (40 μl), which were charged with 2.2 mg of *sym*-OHA (12 μmol) and 4.4 mg of Pt/HM30A, at 150–185°C for 0.15–2 h. The apparatus used for the reactions in microreactors was the Mettler DSC 27HP. The liquid products were also recovered by washing with acetone after the reaction and were analyzed by GC and GC-MS.

The gaseous products were analyzed quantitatively using a Perkin-Elmer Autosystem GC. Two detectors, a flame ionization detector (FID) and a thermal conductivity detector (TCD), were used to analyze the gas composition. The GC columns used were a 6 feet long, 1/8 inch diameter stainless steel column packed with 80/100 Chemipack C 18 for FID and a 15 feet long, 1/8 inch diameter stainless steel column packed with 60/80 Carboxen 1000 (Supelco) for TCD. The compounds in the liquid products were identified by an HP 5890 Series II GC coupled with an HP 5971A mass selective detector (MSD) and quantified by a Perkin-Elmer GC 8500 equipped with an FID. The column was a 30 m, 0.25 mm i.d., DB-17 fused silica

capillary column (50% phenyl–50% methyl polysiloxane) with a film thickness of 0.25 μm. More details for the analytical procedures may be found elsewhere [20]. In order to calibrate the GC peak areas of products, the response factors of the major components in the liquid products were experimentally determined by using pure compounds, and they were found to be similar to each other. Therefore, GC peak areas were used directly in all the mass balance calculation. The mass balance was over 95% for runs with conversion below 55%, and decreased somewhat when conversion was above 55%. Carbon deposition on the catalyst determined from TGA was generally insignificant except for runs under severe conditions such as at 300°C for 1 h, where the carbon accounted for about 2 wt% of the starting reagent.

3. Results and discussion

3.1. Acidity of catalysts

The acidity of all the catalysts were characterized by *n*-BA desorption using TGA and DSC. Fig. 1 shows the thermal analysis results for HY. DSC curve shows several endothermic peaks: a clear low-temperature peak near 100°C, a shallow peak near 200°C, a large peak at 405°C, and a shoulder peak near 440°C. It is known that the stronger the acidity of the acid sites, the higher the temperature or energy is required to desorb the base (*n*-BA). It is clear that HY possesses active sites with different strength. The peak near 100°C may be due to the desorption of physisorbed *n*-BA, and *n*-BA adsorbed on weak acid sites [21]. As mentioned earlier, trace amount of water might have re-adsorbed on the catalyst; thus, the peak near 100°C might also be due to the desorption of physisorbed water. This is especially true for highly hydrophilic catalysts. On the other hand, the high-temperature peaks above ca. 300–400°C are regarded as being attributed to the desorption from strong acid sites. DTG shows similar results except that the peak near 100°C is not as clear as that in DSC. It can be seen that for HY the results from DTG compared fairly well with that from DSC.

The DSC and TGA curves of *n*-BA desorption from all the catalysts are presented in Figs. 2 and 3, respectively. Fig. 4 summarizes the acidity of catalysts determined from the amount of *n*-BA desorbed (from the TGA measurements) at three temperature ranges (100–240, 240–340, and 340–500°C). The three temperature ranges were chosen to represent acid sites with different strengths. It was assumed that the weight loss below 100°C (about 1–1.5 wt% of the saturated catalysts) was due to the desorption of physisorbed base, and thus only the amount of *n*-BA desorbed above 100°C was considered in the calculation of acidity. The temperature limit was set at 500°C because it was suggested that the weight loss above 500°C

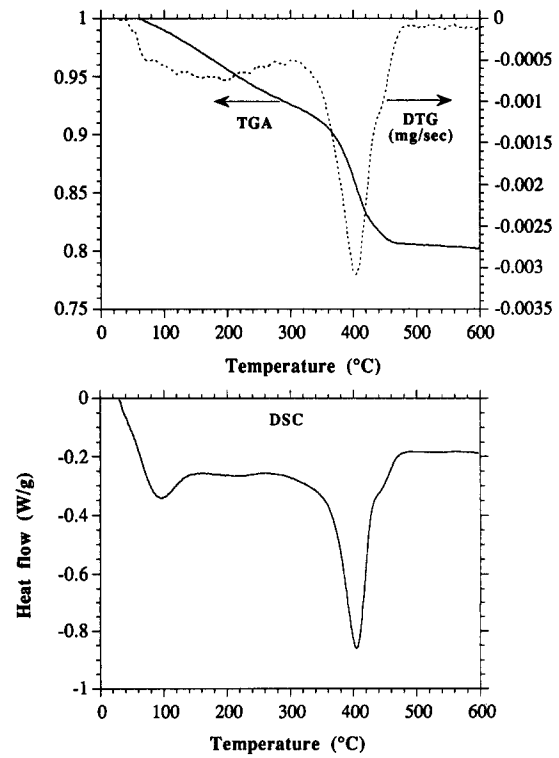

Fig. 1. TGA, DTG, and DSC curves of temperature-programmed desorption of *n*-butylamine from HY.

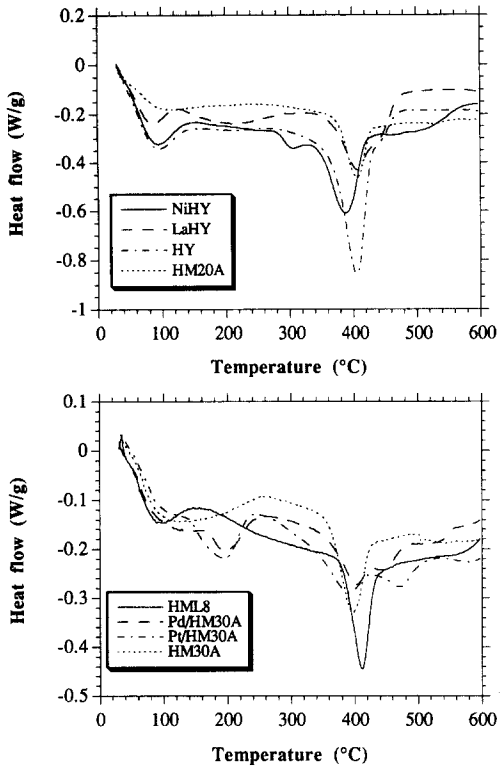

Fig. 2. DSC curves of *n*-butylamine desorption from seven catalysts.

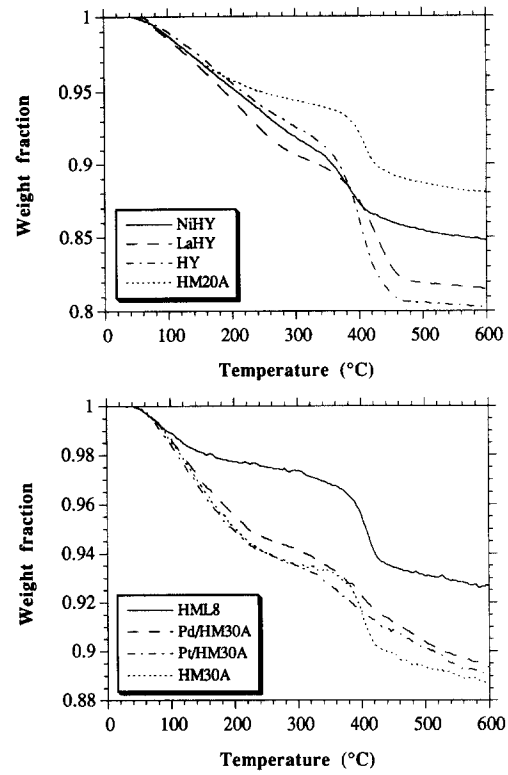

Fig. 3. TGA curves of *n*-butylamine desorption from seven catalysts.

may also be due to the dehydroxylation of the catalysts [21].

There are several observations from the thermal analysis data. First, Fig. 3 showed that the amount of *n*-BA desorption weight loss from all the Y-zeolites was greater than that from all the mordenites at all temperatures, indicating that the Y-zeolites have both higher acid strength and more acid sites than the mordenites. The total acidity for the catalysts is: HY > LaHY > NiHY > HM20A > HM30A > Pd/HM30A ≈ Pt/HM30A > HML8. Second, compared to the other seven catalysts, HY has more strong acid sites judged from the enormous endothermic heat flow (Fig. 2) or sharp weight loss (Fig. 3) in the 340–500°C range. Third, HML8 only possesses a small number of weak sites, in fact the least among the eight catalysts; however, it has similar amount of strong sites as HM30A has, although they have different SiO_2/Al_2O_3 ratio. Fourth, the two noble metal loaded mordenites (Pt/HM30A and Pd/HM30A) have quite similar acidity, and they possess fewer strong sites than HM30A. Fifth, among the three Y-zeolites, LaHY has slightly more weak sites than the other two, but it has fewer strong sites than HY. NiHY has similar amount of weaker sites but much fewer strong sites than HY and LaHY.

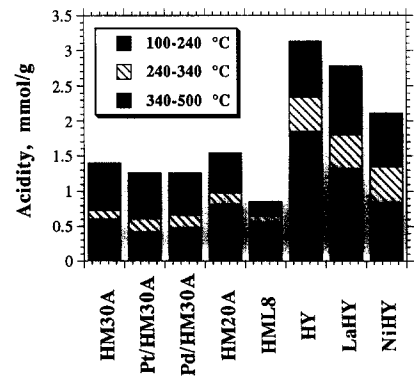

Fig. 4. Acidity of catalysts determined by using TGA of *n*-butylamine desorption.

3.2. Effectiveness of catalysts

3.2.1. HML8, HM20A, HM30A, HY, LaHY, and NiHY

3.2.1.1. Isomerization of sym-OHP. HML8 was studied more extensively than other catalysts in this work, because it was found to be the best among several zeolitic catalysts in our previous work at 250°C for 2 h [13,14]. Table 1 presents the results of *sym*-OHP isomerization over HML8 with *sym*-OHP as the starting material at three different temperatures (200, 250, and 300°C) under N_2. The results over five other catalysts (HM20A, HM30A, HY, LaHY, and NiHY) are shown in Table 2.

The major reaction of interest in this work is the isomerization of *sym*-OHP to *sym*-OHA. Fig. 5 shows the temporal plot of *sym*-OHP conversion and selectivity towards *sym*-OHA plus 1,2,3,4-THA. Table 1 and Fig. 5 indicate that HML8 is an effective catalyst for this reaction because it could afford over 90% selectivity with reasonable conversion (about 50%). In order to approach equilibrium conditions, relatively long residence times have been employed, e.g. 22 h at 200°C, 4 h at 250°C, and 1 h at 300°C. It is clear from Table 1 that the reactions seemed to have reached the asymptotic equilibrium after 22 h at 200°C, 2 h at 250°C, and 0.25 h at 300°C. In other words, the yield of *sym*-OHA reached its maximum at those reaction conditions, and longer reaction times at 250 and 300°C only served to decrease the *sym*-OHA yield because of enhanced competitive side-reactions or secondary reactions such as ring-opening cracking and subsequent dealkylation (to form mainly alkyltetralins), conventional ring-contraction isomerization, and dehydrogenation. The selectivity towards *sym*-OHA suffered severely when the reaction temperature was increased to 300°C as shown in Fig. 5, when side-reactions became significant.

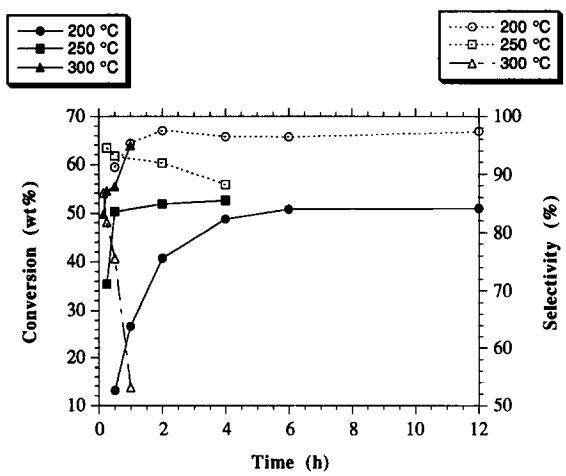

Fig. 5. Temporal plot of *sym*-OHP conversion and selectivity towards *sym*-OHA plus 1,2,3,4-THA over HML8 at three different temperatures (200, 250, and 300°C) under N_2.

A kinetic analysis of the 200–300°C data over HML8 was performed assuming the first-order relation shown in Eq. (1),

$$-\frac{dC}{dt} = kC \tag{1}$$

where C is the reactant concentration (mol l^{-1}), t is the reaction time (h), and k is the first-order rate constant (h^{-1}). The rate constant k was determined by using Eq. (2),

$$k = \frac{1}{t} \ln \frac{1}{1-X} \tag{2}$$

where X is the fractional conversion of *sym*-OHP. Then the rate constant was correlated by the Arrhenius law as shown in Eq. (3),

$$k = Ae^{-E_a/RT} \tag{3}$$

where A (h^{-1}) is the frequency (or preexponential) factor, E_a is the apparent activation energy (kcal/mol), and R is the gas constant (kcal mol^{-1} K^{-1}). The apparent E_a and A values determined from the Arrhenius plot are as follows:

$$E_a = 14.1 \text{ kcal/mol and } A = 9.87 \times 10^5 \text{ h}^{-1} \tag{4}$$

The low E_a value derived for HML8 coupled with the fact that it has high selectivity towards *sym*-OHA suggests that HML8 is a promising

catalyst for the isomerization of *sym*-OHP into *sym*-OHA.

The effect of SiO_2/Al_2O_3 ratio of mordenites was examined by using HM20A and HM30A in addition to HML8. Recall that the SiO_2/Al_2O_3 molar ratios of HML8, HM20A, and HM30A are 17, 21, and 38, respectively. Among the three mordenites, the catalyst that has lower acidity and SiO_2/Al_2O_3 ratio (HML8) displayed the best selectivity to *sym*-OHA but the lowest activity. Comparing Tables 1 and 2, we can see that at 200°C these three mordenites reacted comparably near the pseudo-equilibrium condition; this could be seen from the similar conversion level (52–53%), selectivity (97–98%), and *sym*-OHA to *sym*-OHP ratio (1.30–1.35). However, at a higher temperature, 250°C, these three mordenites behaved slightly different. In general, the catalytic selectivity towards *sym*-OHA suffered due to more significant side-reactions when the temperature was increased. Thus, comparisons of selectivity must be made at similar conversion levels. One example could be seen at similar conversion level, 51.9%, where the selectivity is 91.9 and 83.5% for HML8 and HM30A, respectively. Among the three mordenites, HM20A, which also has the highest acidity, exhibited the highest activity for *sym*-OHP conversion but the lowest selectivity towards *sym*-OHA plus THA. The catalytic effectiveness is in the order HM20A > HM30A > HML8 for activity and HML8 > HM30A > HM20A for selectivity, respectively. In short, although there is no apparent linear relationship between the activity/selectivity and SiO_2/Al_2O_3 molar ratios for *sym*-OHP isomerization, there seems to be a relationship between the activity/selectivity and acidity. All three mordenites show promising results at 200°C in terms of both activity and selectivity, but HM30A and HM20A are not as selective as HML8 at 250°C.

Among the three Y-zeolites, best selectivity to *sym*-OHA was achieved with the catalyst (NiHY) that has lower acidity and lower content of stronger acid sites (corresponding to *n*-BA desorption in 340–500°C). HY was also an effective catalyst at 200°C because it could afford 96% selectivity with reasonable conversion (about 51%). LaHY performed very similarly to HY at 250°C as shown in Table 2 in that they had high activity but the selectivity to anthracene derivatives was low. In fact, among the six catalysts discussed so far, HY and LaHY had the highest activity; their high activity was attributed to their higher acid strength and more acid sites than the other four catalysts (see Fig. 4). However, the nickel ion-exchanged Y zeolite, i.e. NiHY, is a promising catalyst, which showed a high selectivity and reasonable activity at 250°C. Although NiHY also has stronger acidity than the mordenites, its selectivity did not suffer so much as HY and LaHY did at 250°C. This seems to suggest that NiHY has the appropriate acidity and catalyst structure required to enhance the desired isomerization reactions without losing too much activity. In addition, the fact that HML8 has the lowest acidity and highest selectivity suggests that the desired acidic characteristics for the isomerization reactions over HML8 and NiHY are different.

The catalytic selectivity towards *sym*-OHA decreases with increasing conversion after the pseudo-equilibrium stage has been reached. Fig. 6 presents the plots of selectivity towards *sym*-OHA plus 1,2,3,4-THA versus *sym*-OHP conversion for the six catalysts in Tables 1 and 2.

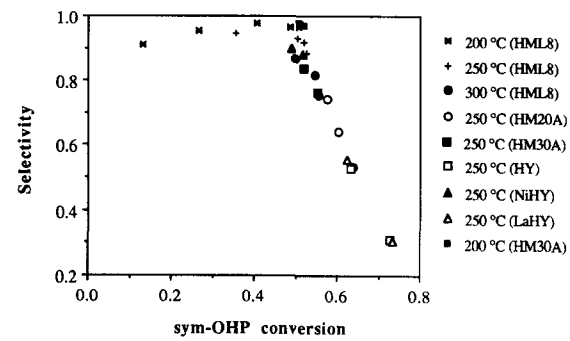

Fig. 6. Selectivity towards *sym*-OHA plus 1,2,3,4-THA versus *sym*-OHP conversion plots for six catalysts.

Table 1
sym-OHP isomerization over HML8 with *sym*-OHP as the starting material at three temperatures under N_2 in tubing bomb reactors

Expt. no.	Temp. (°C)	Time (h)	Products (wt% of feed)									X [c] (%)	Sel. [d] (%)	Ratio $\frac{sym-OHA}{sym-OHP}$
			sym- OHA	THA [a]	*sym*- OHP	*asym*- OHP [a]	9,10- DHP [a]	HHP [a]	THP [a]	Phen. [a]	Others [b]			
		– [e]	2.90		91.04	0.32	2.67	1.74	0.77	0.07	0.50			0.03
PS6	200	0.50	14.70	0.11	77.99	0.35	2.78	0.43	1.40	0.15	2.10	13.1	91.2	0.19
PS8	200	1.00	28.10	0.21	64.38	0.34	2.59	0.52	1.20	0.20	2.45	26.7	95.3	0.44
PS9	200	2.00	42.30	0.26	50.35	0.36	2.57	0.22	1.16	0.20	2.58	40.7	97.5	0.84
PS14	200	4.00	49.64	0.33	42.25	0.35	2.60	0.04	1.21	0.17	3.41	48.8	96.5	1.17
PS15	200	6.00	51.44	0.45	40.20	0.33	2.54	0.04	1.29	0.16	3.55	50.8	96.4	1.28
PS41	200	12.0	52.15	0.42	40.07	0.35	2.62	0.04	1.24	0.17	2.94	51.0	97.4	1.30
PS49	200	22.0	52.18	0.58	40.00	0.33	2.50	0.04	1.29	0.23	2.85	51.0	96.6	1.30
PS10	250	0.25	35.90	0.48	55.62	0.36	2.53	0.51	1.21	0.20	3.18	35.4	94.5	0.65
PS1	250	0.50	48.76	1.00	40.70	0.30	2.53	0.12	1.67	0.33	4.59	50.3	93.1	1.20
PS3	250	2.00	49.32	1.30	39.11	0.22	2.23	0.03	1.65	0.49	5.65	51.9	91.9	1.26
PS18	250	4.00	47.74	1.56	38.42	0.13	1.95		1.88	0.75	7.57	52.6	88.2	1.24
PS13	300	0.15	44.96	1.21	41.20	0.20	2.20	0.12	2.03	0.60	7.48	49.8	86.8	1.09
PS7	300	0.25	45.50	1.95	36.58	0.10	1.50	0.27	2.26	0.80	11.04	54.5	81.8	1.24
PS4	300	0.50	42.67	2.13	35.64	0.15	1.75	0.12	3.70	1.12	12.72	55.4	75.6	1.20
PS5	300	1.00	33.62	3.20	27.19	0.10	0.80	0.12	3.98	1.53	29.46	63.9	53.1	1.24

[a] THA = 1,2,3,4-tetrahydroanthracene; *asym*-OHP = 1,2,3,4,4a,9,10,10a-octahydrophenanthrene; 9,10-DHP = 9,10-dihydrophenanthrene; HHP = 1,2,3,4,4a,10a-hexahydrophenanthrene; THP = 1,2,3,4-tetrahydrophenanthrene; Phen. = phenanthrene.
[b] Others include products of ring-contraction isomerization and ring-opening cracking and subsequent dealkylation.
[c] X = conversion of *sym*-OHP (wt% of feed).
[d] Selectivity to *sym*-OHA plus THA, defined as the percentage of *sym*-OHP conversion.
[e] This row presents the purity of as-received *sym*-OHP.

Table 2
sym-OHP isomerization over various catalysts with *sym*-OHP as the starting material at two temperatures under N_2 in tubing bomb reactors

Expt. no.	Catalyst type	Temp. (°C)	Time (h)	Products (wt% of feed)									X [a] (%)	Sel. [b] (%)	Ratio $\frac{sym-OHA}{sym-OHP}$
				sym-OHA	THA	*sym*-OHP	*asym*-OHP	9,10-DHP	HHP	THP	Phen.	Others			
			– [c]	2.90		91.04	0.32	2.67	1.74	0.77	0.07	0.50			0.03
PS51	HM20A	200	2.0	53.25	0.22	39.63	0.35	1.82	0.02	1.55	1.03	2.13	51.4	98.0	1.34
PS52	HM30A	200	2.0	52.49	0.30	40.35	0.34	2.60	0.04	1.42	0.23	2.23	50.7	97.8	1.30
PS42	HM30A	200	12.0	52.57	0.64	39.03	0.30	2.39	0.14	1.40	0.31	3.22	52.0	96.7	1.35
PS50	HY	200	2.0	52.02	0.67	39.92	1.15	0.52	0.02	1.37	1.30	3.03	51.1	96.1	1.30
PS11	HM20A	250	0.5	43.03	2.69	33.38	1.92	0.60	0.25	3.88	1.50	12.75	57.7	74.3	1.29
PS12	HM20A	250	1.0	38.64	2.88	30.77	2.86	0.59	0.27	4.17	1.41	18.41	60.3	64.1	1.26
PS16	HM30A	250	0.5	44.47	1.72	39.19	0.21	1.55	0.14	2.34	1.05	9.33	51.9	83.5	1.13
PS17	HM30A	250	1.0	42.87	2.06	35.90	0.12	1.20	0.11	2.54	1.29	13.91	55.1	76.2	1.19
PS19	HY	250	0.5	33.22	2.92	27.82	4.35	0.40		5.13	1.20	24.95	63.2	52.6	1.19
PS20	HY	250	1.0	22.14	3.37	18.36	4.88	0.39		5.30	1.16	44.41	72.7	31.1	1.21
PS21	LaHY	250	0.5	34.86	2.72	28.73	3.93	0.45		4.75	1.34	23.21	62.3	55.7	1.21
PS22	LaHY	250	1.0	21.80	3.60	17.63	3.76	0.39		5.45	1.20	46.17	73.4	30.7	1.24
PS23	NiHY	250	0.5	45.87	0.94	42.11	1.03	0.47	0.05	4.29	1.61	3.63	48.9	89.7	1.09
PS24	NiHY	250	1.0	46.88	1.24	39.58	1.52	0.48	0.07	4.50	1.48	4.25	51.5	87.9	1.18

[a] X = conversion of *sym*-OHP (wt% of feed).
[b] Selectivity to *sym*-OHA plus THA, defined as the percentage of *sym*-OHP conversion.
[c] This row presents the purity of as-received *sym*-OHP.

The selectivity for the catalysts at 250°C is: HML8 > NiHY > HM30A > HM20A > LaHY ≈ HY. The conversion level is about 50% near pseudo-equilibrium stage. The selectivity towards anthracene derivatives is high (above 90%) and is not very sensitive to the conversion level when the conversion is below 50%. However, the selectivity decreases almost linearly with increasing conversion above 50%. For example, a 10% conversion increase above 50% will cause about a 25% selectivity decrease. The selectivity decrease was due to significant side reactions or secondary reactions. In short, it is important to identify the equilibrium state because further reaction beyond the equilibrium stage is not beneficial to the production of *sym*-OHA.

The observed reactivities of the impurities, such as 9,10-DHP and 1,2,3,4,4a,10a-HHP, in *sym*-OHP are discussed briefly below. The purity analysis of the starting material (presented in Table 1) is important, because without this information the impurities may be mistaken as products. When HML8 was used (Table 1), 9,10-DHP did not react to a great extent except under severe conditions, e.g. 300°C for 1 h, and the main reaction of 9,10-DHP was believed to be dehydrogenation to phenanthrene under current reaction conditions. The supporting evidence is that the sum of 9,10-DHP and phenanthrene was relatively constant (about 2.8) for most of the reaction conditions. Other researchers also suggested the hydrogenation of 9,10-DHP to 1,2,3,4-THP [22] and *asym*-OHP [3] under hydroprocessing conditions. However, these hydrogenation reactions are less likely over HML8 judging from the deficiency of hydrogen and the overall product distribution of 1,2,3,4-THP and *asym*-OHP. In contrast to HML8, when high-acidity catalysts such as HY and HM20A (Table 2) were used, 9,10-DHP reacted more quickly and was accompanied by significant yields of *asym*-OHP, 1,2,3,4-THP, and phenanthrene. They appeared to possess a much higher ability of promoting dehydrogenation as well as hydrogenation than HML8 and HM30A. The hydrogenation of 9,10-DHP to 1,2,3,4-THP and *asym*-OHP, which is a less likely reaction over HML8, became apparent with HY and HM20A. This implies that some reaction pathways depend on the type of catalysts used. In contrast to 9,10-DHP, 1,2,3,4,4a,10a-HHP reacts quickly even over HML8 at a low temperature, 200°C. The main reactions of 1,2,3,4,4a,10a-HHP include dehydrogenation to 1,2,3,4-THP, and ring-contraction isomerization and ring-opening cracking.

3.2.1.2. Isomerization of sym-OHA. Some experiments using pure *sym*-OHA (rather than *sym*-OHP) as starting material were also performed to check the reversibility of the ring-shift isomerization and to confirm the experimentally obtained pseudo-equilibrium composition (Table 1). The results of *sym*-OHA isomerization over HML8 with *sym*-OHA as the starting material at three temperatures under N_2 environment are given in Table 3. The results demonstrate the reversibility of the ring-shift isomerization. Furthermore, it was shown again that HML8 was quite selective for the ring-shift isomerization except under severe conditions. Table 3 indicates that the reactions seemed to have reached pseudo-equilibrium after 4 h at 200°C, 0.5 h at 250°C, and 0.15 h at 300°C judging from the fact that the yield of *sym*-OHP reached its maximum at those reaction conditions. The pseudo-equilibrium compositions of *sym*-OHA and *sym*-OHP and their ratios reported in Table 3 are very close to those in Table 1. For example, the equilibrium ratio is not sensitive to the reaction temperature and is close to 1.3.

The desirable reaction conditions are summarized as follows. From the data in Table 1, Table 2, and Table 3, for the HML8 catalyst, in terms of reaction rate for *sym*-OHP conversion alone, it appears desirable to operate the reaction at a high temperature level such as 300°C. However, the selectivity towards *sym*-OHA drops rapidly upon increasing temperature to 300°C due to significant side-reactions. Taking

Table 3
sym-OHA isomerization over HML8 with *sym*-OHA as the starting material at three temperatures under N_2 in tubing bomb reactors

Expt. no.	Temp. (°C)	Time (h)	Products (wt% of feed)						X [a] (%)	Sel. [b] (%)	Sel. [c] (%)	Ratio $\frac{sym-OHA}{sym-OHP}$
			sym-OHA	THA	*sym*-OHP	HHP	THP	Others				
PS27	200	1.00	61.44	0.23	35.52	0.18	0.08	2.54	38.6	92.1	92.8	1.73
PS28	200	4.00	55.07	0.40	41.22	0.14	0.10	3.07	44.9	91.7	92.3	1.34
PS33	200	8.00	55.42	0.39	40.56	0.16	0.09	3.38	44.6	91.0	91.5	1.37
PS25	250	0.25	56.18	0.67	37.95	0.25	0.20	4.75	43.8	86.6	87.6	1.48
PS26	250	0.50	53.36	0.76	40.69	0.27	0.30	4.62	46.6	87.2	88.5	1.31
PS32	250	2.00	51.38	1.04	39.91	0.19	0.57	6.91	48.6	82.1	83.6	1.29
PS29	300	0.15	50.91	1.26	39.15	0.23	0.92	7.53	49.1	79.8	82.1	1.30
PS30	300	0.25	45.97	1.67	36.39	0.18	1.57	14.22	54.0	67.4	70.6	1.26
PS31	300	0.50	40.65	2.28	32.36	0.16	2.52	22.03	59.4	54.5	59.0	1.26

[a] X = conversion of *sym*-OHA (wt% of feed, *sym*-OHA).
[b] Selectivity to *sym*-OHP, defined as the percentage of *sym*-OHA conversion.
[c] Selectivity to *sym*-OHP plus HHP and THP, defined as the percentage of *sym*-OHA conversion.

both rate and selectivity into consideration, 250°C for 0.5 h appears to be a desirable condition for the *sym*-OHP isomerization over HML8. Other catalysts with higher acidity (such as HM20A, HM30A, and HY) show both high selectivity and promising conversion at 200°C, and thus could be desirable catalysts for use at 200°C. However, appropriate reaction time (less than 0.5 h) should be used when these high-acidity catalysts are applied at higher temperature such as 250°C, in order to obtain high selectivity products by minimizing undesirable secondary and side reactions.

3.2.2. Pt / HM30A and Pd / HM30A

The motivation of using these two noble metal loaded mordenites on the ring-shift isomerization comes from the promising activity and selectivity observed in our study on conformational isomerization of *cis*-decalin using the same catalysts [23]. It was found that Pt- and Pd-loaded mordenites are very effective catalysts under H_2 atmosphere for the conformational isomerization of *cis*-decalin even at 200°C. Table 4 presents the results of isomerization over Pt/HM30A and Pd/HM30A with *sym*-OHP or *sym*-OHA as the starting material at 200°C under 0.79 MPa of H_2 or N_2 in tubing bomb reactors.

3.2.2.1. Isomerization of sym-OHP.

Mordenites loaded with noble metal exhibits much higher activity but lower selectivity towards hydrogenated anthracenes. The effect of noble metals can be seen by comparing the results of HM30A (PS42, in Table 2) and those of Pt- and Pd-loaded HM30A (PS47 and PS48, respectively, see Table 4). The activity for *sym*-OHP conversion is: Pd/HM30A > Pt/HM30A > HM30A. The lower selectivity towards *sym*-OHA for both Pd/HM30A and Pt/HM30A is due to the significant dehydrogenation reactions to form THA and THP or even phenanthrene under N_2. The results are not beyond expectation because both Pt and Pd are well known active metals for dehydrogenation and hydrogenation. Hydrogenation was not apparent because of the H_2 deficient environment, since reactions were performed under N_2. The dehydrogenation activity drops in the order Pd > Pt.

Changing the gas environment from N_2 to H_2 (see Table 4) significantly affects the final product distribution because the dehydrogenation under N_2 was replaced with hydrogenation under H_2. Fig. 7 presents the temporal plots of major products from *sym*-OHP isomerization using Pt/HM30A and Pd/HM30A at 200°C under excess H_2 (8 mmol). Fig. 7 provides information about the reaction pathways. For

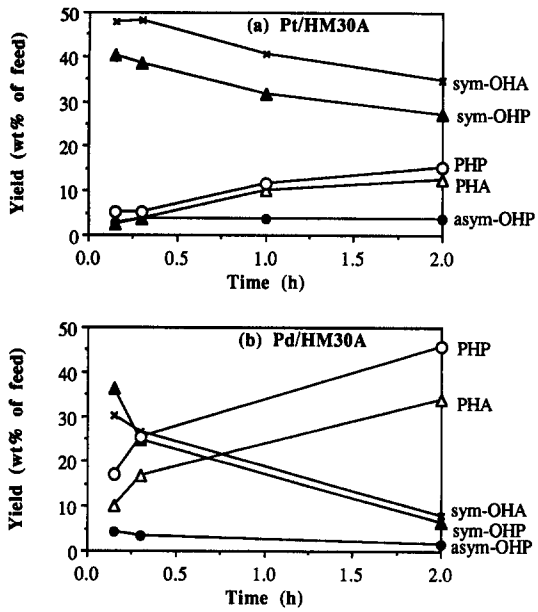

Fig. 7. Temporal plots of major products from *sym*-OHP isomerization at 200°C under H_2.

example, for the Pt/HM30A catalyst, it can be seen that *sym*-OHA was the primary product; its yield reached a maximum at 0.3 h and then decreased due to enhanced hydrogenation reactions. On the other hand, perhydroanthracene (PHA) and perhydrophenanthrene (PHP) appeared to be the secondary products resulting from hydrogenation of OHA or OHP. Table 4 shows that for Pt/HM30A after 0.3-h reaction time, the ratio of *sym*-OHA to *sym*-OHP approached a constant value of 1.28, which was very close to the pseudo-equilibrium mole ratio determined from the study of HML8, HM20A, HM30A, and HY at 200°C (Tables 1 and 2). All these results suggest that *sym*-OHA formation is the major primary reaction, and hydrogenation of OHP and OHA did not occur until *sym*-OHA and *sym*-OHP reached pseudo-equilibrium. In addition, it was demonstrated that

Table 4
Ring-shift isomerization over noble metal loaded mordenites with *sym*-OHP or *sym*-OHA as the starting material at 200°C under H_2 or N_2 in tubing bomb reactors

Catalyst		Pt/HM30A						Pd/HM30A				
Time (h)	– [a]	0.30	0.15	0.30	1.00	2.00	2.00	0.30	0.15	0.30	2.00	2.00
Starting reactant		OHP	OHP	OHP	OHP	OHP	OHA	OHP	OHP	OHP	OHP	OHA
0.79 MPa N_2 or H_2		N_2	H_2	H_2	H_2	H_2	H_2	N_2	H_2	H_2	H_2	H_2
Expt. no.		PS47	PS45	PS43	PS36	PS39	PS38	PS48	PS46	PS44	PS37	PS40
X (%) [b]	– [a]	58.0	50.9	52.8	59.3	63.9	62.8	61.1	54.9	66.2	84.6	96.0
Products (wt% of feed)												
sym-OHA	2.90	42.52	47.82	48.07	40.62	34.76	37.21	38.10	30.17	26.53	8.01	4.03
THA		7.77				0.20	0.05	9.00				
PHA [c]			2.57	3.70	9.94	12.63	12.06		10.00	16.72	33.77	40.11
sym-OHP	91.04	33.07	40.16	38.28	31.72	27.13	29.44	29.99	36.17	24.80	6.47	3.21
asym-OHP	0.32	1.14	2.62	3.53	3.67	3.65	3.61	1.95	4.23	3.47	1.55	0.82
9,10-DHP	2.67	0.71	0.01		0.03	0.13	0.14	1.47	0.01			
HHP	1.74	0.02	0.02	0.06	0.06	0.03		0.02	0.02	0.08		
THP	0.77	10.45			0.12	0.91	0.36	12.66				
Phenanthrene	0.06	3.35						5.20				
PHP [c]		0.08	5.25	5.06	11.53	15.12	13.24	0.07	16.94	25.34	45.85	47.40
Others	0.50	0.89	1.55	1.30	2.31	5.44	3.89	1.54	2.46	3.06	4.35	4.43
Selectivity [d] (%)		81.7	93.3	92.6	80.3	69.9		72.4	67.9	60.9	46.0	
Selectivity [e] (%)							46.9					3.3
Selectivity [f] (%)							74.5					53.6
sym-OHA/*sym*-OHP	0.03	1.29	1.19	1.26	1.28	1.28	1.26	1.27	0.83	1.07	1.24	1.26

[a] This column presents the purity of as-received *sym*-OHP.
[b] *X* = conversion of *sym*-OHP or *sym*-OHA (wt% of feed).
[c] PHA = perhydroanthracene; PHP = perhydrophenanthrene.
[d] Selectivity to *sym*-OHA plus THA and PHA, defined as the percentage of *sym*-OHP conversion.
[e] Selectivity to *sym*-OHP, defined as the percentage of *sym*-OHA conversion.
[f] Selectivity to hydrogenated phenanthrenes, defined as the percentage of *sym*-OHA conversion.

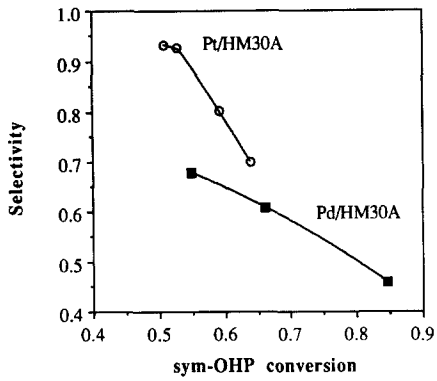

Fig. 8. Selectivity towards *sym*-OHA plus 1,2,3,4-THA versus *sym*-OHP conversion plots for ring-shift isomerization over Pt/HM30A and Pd/HM30A at 200°C under H_2.

Pt/HM30A shows promising activity and selectivity at 200°C under H_2. Optimal products may be reached in a short period of time, e.g. 0.15–0.3 h. Longer reaction time under H_2 beyond the pseudo-equilibrium stage is not beneficial to the production of *sym*-OHA, due to pronounced hydrogenation to form further hydrogenation products such as PHA and PHP.

The other noble metal catalyst, Pd/HM30A, showed slightly different results. Fig. 8. presents the selectivity towards *sym*-OHA plus 1,2,3,4-THA versus *sym*-OHP conversion plots over Pt/HM30A and Pd/HM30A at 200°C under H_2 (see Table 4). Pd again shows higher activity but lower selectivity towards hydrogenated anthracenes. Its superior hydrogenation ability might have changed the reaction pathways. For example, instead of being a secondary product only, PHP might as well be a primary product too. The hydrogenation and isomerization reactions might have proceeded in parallel instead of in series for Pd/HM30A under H_2. The supporting evidence is that the ratio of *sym*-OHA to *sym*-OHP did not approach the pseudo-equilibrium mole ratio until very late in the reaction when *sym*-OHP was almost completely consumed. The results suggest that such a strong ability of dehydrogenation and hydrogenation might make Pd a less favorable catalyst for the ring-shift isomerization of *sym*-OHP.

3.2.2.2. Isomerization of sym-OHA. The results of *sym*-OHA isomerization over Pt/HM30A and Pd/HM30A with *sym*-OHA as the starting material under H_2 environment, are also given in Table 4. The reversibility of the ring-shift isomerization was confirmed again. Pd again shows much higher activity (96% conversion) but lower selectivity towards hydrogenated phenanthrenes. Although the product compositions from Pt/HM30A and Pd/HM30A are quite different, the ratios of *sym*-OHA to *sym*-OHP are close (1.26), implying that the reactions have approached the pseudo-equilibrium mole ratio.

To further understand the effectiveness of Pt/HM30A, reactions were carried out in hermetically sealed aluminum cells (40 μl) at lower temperatures (150–185°C). Fig. 9 presents an expanded retention time window of four GC

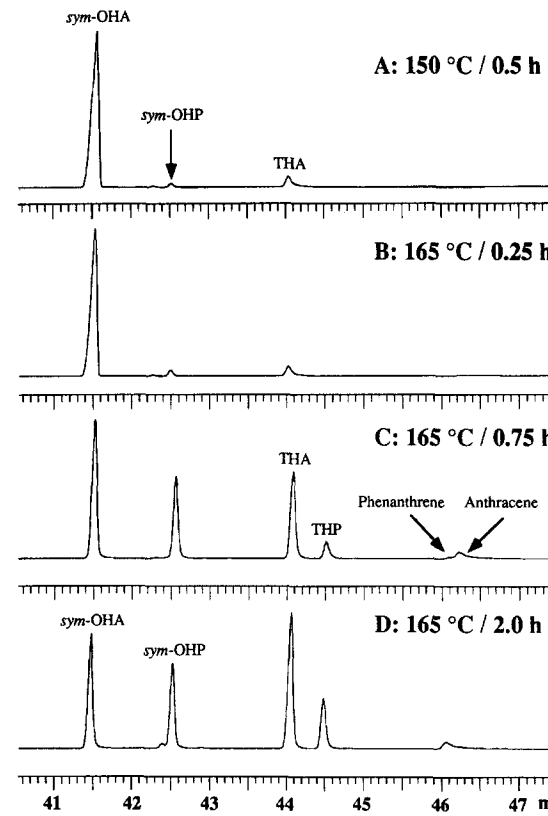

Fig. 9. Expanded retention time window of GC profiles for four liquid products from *sym*-OHA over Pt/HM30A: (A) 150°C/0.5 h; (B) 165°C/0.25 h; (C) 165°C/0.75 h; (D) 165°C/2.0 h.

profiles for the liquid products at 150 and 165°C. In the early stage of the reaction, for example, at 150°C for 0.5 h and 165°C for 0.25 h, the yield of dehydrogenation products such as 1,2,3,4-THA was higher than the isomerization product (*sym*-OHP). As reactions proceed, *sym*-OHP increases progressively, and the formation of *sym*-OHP is always accompanied by more dehydrogenation products such as 1,2,3,4-THA and 1,2,3,4-THP or even phenanthrene under N_2. As can be seen from Fig. 9, dehydrogenation and isomerization reactions seemed to proceed in parallel starting from the early stage of reactions with 1,2,3,4-THA, with *sym*-OHP as the primary product and other dehydrogenation products as the secondary ones. *sym*-OHA and *sym*-OHP quickly approached pseudo-equilibrium as shown in Table 5, which shows the ratios of *sym*-OHA to *sym*-OHP as a function of reaction conditions. The ratios of *sym*-OHA to *sym*-OHP for the temperature range 165–185°C, all approached a similar constant value of about 1.30, which was also the pseudo-equilibrium mole ratio determined from catalysts such as HML8 and HM30A at 200°C. The experimental data again show that the equilibrium ratio is not sensitive to the reaction temperature and catalysts used. Recall that the data in Table 5 were obtained without using any solvent; it implies that for very active catalysts such as Pt/HM30A, the solvent has little effect on the equilibrium ratio of *sym*-OHA to *sym*-OHP.

It was demonstrated that Pt/HM30A shows promising activity and selectivity at temperature as low as 165°C under N_2. However, due to the catalyst's high dehydrogenation ability under N_2, optimal reaction time should be used if the products of interest are isomerization compounds. The high dehydrogenation ability of Pt/HM30A could be demonstrated by another example. In an experiment with 9,10-DHP as the sole reactant at 200°C under N_2 for 0.3 h, it was found that the only main (almost exclusive) product was phenanthrene due to dehydrogenation of 9,10-DHP.

3.3. Molecular mechanics calculation of equilibrium concentrations

The equilibrium compositions of *sym*-OHP and *sym*-OHA at three temperatures were calculated to establish the theoretical upper limit of the catalytic conversion. Calculations on the various conformers present in an equilibrium mixture containing only *sym*-OHA and *sym*-OHP were performed. In order to obtain the raw geometries for the molecules and to find the different conformers present, the DELPHI-molecular mechanics program was used with the MM3 force field. The obtained minimized geometries were used as starting points for the MM3 program, using the MM3 force field (both the 1992 versions). Only slight differences were found between the optimized DELPHI- and MM3-geometries. Five and six different conformers were found for *sym*-OHA and *sym*-OHP, respectively, as shown in Fig. 10. Table 6 shows the calculated heats of formation and entropies for the different conformations of *sym*-OHA and *sym*-OHP at 25°C. The literature value of the heat of formation of *sym*-OHA is −8.89 kcal/mol [24]. The good agreement between the literature value (−8.89 kcal/mol)

Table 5
The ratios of *sym*-OHA to *sym*-OHP over Pt/HM30A with *sym*-OHA as the starting material at three temperatures in hermetically sealed aluminum crucibles

Expt. no.	P9	P27	P16	P7	P10	P15	P20	P11	P13	P25	P19
Temp. (°C)	165			175				185			
Time (h)	0.25	0.75	2.0	0.15	0.25	0.5	1.0	0.15	0.25	0.5	0.75
Ratio	36.9	1.77	1.38	3.37	2.23	1.38	1.31	1.48	1.36	1.29	1.29

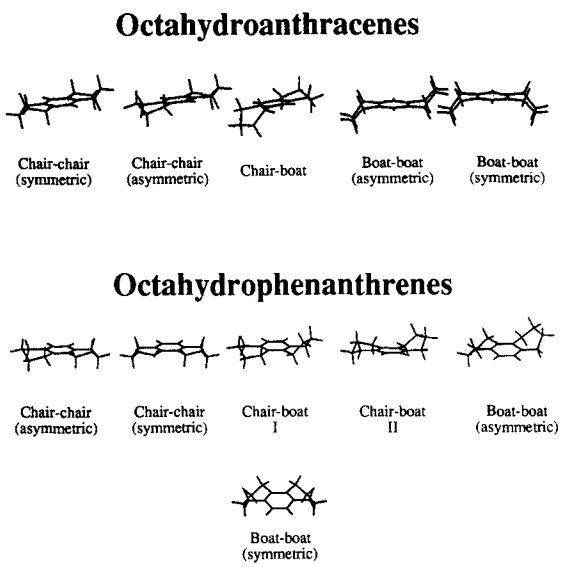

Fig. 10. Different conformers of *sym*-OHA and *sym*-OHP.

and the calculated one (−9.17 kcal/mol, in Table 6) indicates that the MM3 force field should be applicable to problems like these. From these data, the Gibbs free energy of *sym*-OHA and *sym*-OHP at 25°C could be obtained. In a similar fashion, the Gibbs free energies of these compounds at 200, 250, and 300°C were calculated by correcting the heats of formation and entropies in Table 6 for different temperatures. From these free energies, the equilibrium composition of the *sym*-OHA/*sym*-OHP mixture was calculated.

Table 6
The calculated heats of formation and entropies at 25°C

Conformation	ΔH_f (kcal/mol)	S (cal/mol K)
sym-Octahydroanthracene		
Double chair (symmetric)	−9.17	105.54
Double chair (asymmetric)	−9.17	105.54
Boat–chair	−6.08	109.27
Double boat (symmetric)	−3.00	107.48
Double boat (asymmetric)	−3.03	107.47
sym-Octahydrophenanthrene		
Double chair (symmetric)	−7.98	106.33
Double chair (asymmetric)	−7.57	106.89
Boat–chair I	−5.05	108.78
Boat–chair II	−4.83	108.76
Double boat (symmetric)	−1.72	108.82
Double boat (asymmetric)	−1.62	108.71

Table 7
Pseudo-equilibrium composition of the *sym*-OHA/*sym*-OHP mixture

Temperature (°C)	OHA:OHP [a]	Others	OHA/OHP ratio
	From experiments using *sym*-OHP [b]		
200	52.2%:40.0%	7.8%	1.30
250	49.3%:39.1%	11.6%	1.26
300	45.5%:36.6%	17.9%	1.24
	From experiments using *sym*-OHA [c]		
200	55.4%:40.6%	4.0%	1.37
250	51.4%:39.9%	8.7%	1.29
300	46.0%:36.4%	17.6%	1.26
	MM3 calculation [d]		
200	71.9%:28.1%		2.56
250	68.7%:31.3%		2.19
300	66.1%:33.9%		1.95

[a] Other products make up the remainder.
[b] Data from runs with HML8: 22 h at 200°C, 2 h at 250°C, and 0.25 h at 300°C.
[c] Data from runs with HML8: 8 h at 200°C, 2 h at 250°C, and 0.25 h at 300°C.
[d] Assuming the reactants and products include only *sym*-OHP and *sym*-OHA.

Table 7 compares the theoretical MM3 calculations and the pseudo-equilibrium yields from experiments at three temperatures. The theoretical calculation results show that since the isomerization from *sym*-OHP to *sym*-OHA is exothermic, the equilibrium conversion of *sym*-OHP decreases with increasing temperature. The *sym*-OHA yield decreases by about 3% when the reaction temperature was raised by 50°C over the temperature range, 200–300°C. The experimental results also show similar magnitude of decrement. Therefore, a lower reaction temperature is thermodynamically favorable. The results also imply that if very effective catalysts could be found and used under appropriate conditions, the optimal product yields could be approached. Although the absolute values of the calculated yields may also depend on the methods and input parameters, the theoretically calculated equilibrium compositions (in Table 7) are useful and could be used for the evaluation of reaction conditions and the effectiveness of catalysts.

The discrepancy between the calculated data and the experimental results is also noted. The

MM3 calculations indicate that the reaction temperature has a moderate effect on the equilibrium ratio of *sym*-OHA to *sym*-OHP. For example, the ratio changes from 2.56 to 1.95 when the temperature is increased from 200°C to 300°C. However, the experiments show that although the reaction temperature affects the reaction rate and selectivity, the equilibrium ratio is not very sensitive to the reaction temperature. For example, the equilibrium ratios are all close to 1.3 for the temperature range studied. Furthermore, the calculated equilibrium yields of *sym*-OHA are considerably higher than the values experimentally determined using either *sym*-OHP or *sym*-OHA as the starting material (Table 7). The following explanations can be offered for this discrepancy.

First, the calculations assume that *sym*-OHP and *sym*-OHA are the only components in the reaction system. However in the experimental system, both *sym*-OHP and *sym*-OHA can react further to form other compounds, and there are other impurity reactants as well as their by-products; the actual equilibrium state depends on more simultaneous chemical reactions. For the current reaction system, at higher temperatures, e.g. 250°C and 300°C, there are significant side reactions as can be seen from the increasing amount of other products in Table 7. Other simultaneous reactions might include the reactions due to the solvent used (1,3,5-trimethylbenzene) as well. Since many reactions are involved, the composition is a resultant of all the operative reactions and is determined by the thermodynamic equilibrium for the total system. It is possible that the occurrence of such simultaneous reactions have shifted the equilibrium state of *sym*-OHA and *sym*-OHP. Second, the discrepancy may also be due in part to the limitations of the theoretical calculations. The equilibrium composition of the *sym*-OHA/*sym*-OHP mixture was calculated from Gibbs free energies, which were calculated by correcting the heats of formation and entropies in Table 6 for different temperatures. Because of the exponential nature of the relationship between equilibrium constant and Gibbs energy change, the calculated results are highly dependent on the thermodynamic parameters used.

Recall that some experiments were carried out using pure *sym*-OHA (rather than *sym*-OHP, which has some impurities) as starting material. Such experiments also help us to see if better pseudo-equilibrium composition could be obtained by using high purity reactant because side reactions can be reduced. The results (in Table 3) confirm that in general 3–5% higher *sym*-OHA yield was obtained near equilibrium conditions because side reactions were minimized. In this context, it is worthy to mention that the higher equilibrium yield of *sym*-OHA calculated from MM3 method (relative to the experimental value) may imply that there is room for improvement. In other words, higher *sym*-OHA yield could be obtained if side reactions can be minimized.

4. Conclusions

The present study has clearly established that *sym*-OHP can be converted into industrially more useful sym-OHA by zeolite-catalyzed ring-shift isomerization with over 95% selectivity at the conversion level of about 50% at 200–300°C.

The rate and selectivity of the isomerization reactions depended on both the metal and support type of the catalysts. Among the three mordenites, the catalyst that has lower acidity (HML8) displayed the best selectivity to *sym*-OHA but the lowest activity. Among the three Y-zeolites, best selectivity to *sym*-OHA was achieved with the catalyst (NiHY) that has lower acidity and lower content of stronger acid sites. The activity for *sym*-OHP conversion is: Pd/HM30A > Pt/HM30A > HY ≈ LaHY > HM20A > HM30A > HML8 > NiHY.

The catalytic selectivity towards *sym*-OHA decreases with increasing conversion after the pseudo-equilibrium stage has been reached (about 50% conversion). The desirable condi-

tion for the *sym*-OHP isomerization over HML8 was 250°C for 0.5 h. Other catalysts with higher acidity (HM20A, HM30A, and HY) show both high selectivity and promising conversion at 200°C, and thus could be desirable catalysts for use at 200°C. However, relatively short reaction time should be used at 250°C, in order to obtain high selectivity products by minimizing undesirable secondary and side reactions. Pt/HM30A showed promising activity and selectivity at temperature as low as 165°C, and the optimal reaction time is 0.15–0.3 h at 200°C under H_2. Too strong an ability of dehydrogenation and hydrogenation might make Pd/HM30A a less favorable catalyst for the ring-shift isomerization of *sym*-OHP.

The molecular mechanics calculations were performed to establish the equilibrium compositions of *sym*-OHP and *sym*-OHA and were compared to experimental results using eight catalysts including HML8, HM20A, HM30A, Pt/HM30A, Pd/HM30A, HY, LaHY, and NiHY. Both the theoretical calculations and experimental results show that the equilibrium conversion of *sym*-OHP decreases with increasing temperature, and the reaction temperature has a moderate effect on the equilibrium yield of *sym*-OHA. However, the calculated equilibrium yield of *sym*-OHA and its ratio to *sym*-OHP are considerably higher than the experimental values. The experimentally determined equilibrium ratios of *sym*-OHA to *sym*-OHP were not very sensitive to the temperature and catalysts used and were close to 1.3 for runs using either *sym*-OHP or *sym*-OHA as the starting material. The discrepancy may be due to two contributing factors: the side reactions under the experimental conditions and the limitations of theoretical calculations.

Acknowledgements

We are grateful to Professor H.H. Schobert and Professor P.B. Weisz for their encouragement, to Dr. T. Golden and Dr. V. Schillinger for providing the mordenite samples, and to Dr. A. Schmitz of PSU for preparing the noble metal catalysts.

References

[1] C. Song and H.H. Schobert, Fuel Proc. Technol., 34 (1993) 157.
[2] N. Kurata, Kagaku To Kogyo, 60 (1986) 274.
[3] Y. Nakatsuji, T. Kubo, M. Nomura and S. Kikkawa, Bull. Chem. Soc. Jpn., 51 (1978) 618.
[4] H.W. Haynes, Jr., J.F. Parcher and N.E. Helmer, Ind. Eng. Chem. Process Des. Dev., 22 (1983) 401.
[5] S.S. Salim and A.T. Bell, Fuel, 63 (1984) 469.
[6] C. Song, K. Hanaoka, T. Ono and M. Nomura, Bull. Chem. Soc. Jpn., 61 (1988) 3788.
[7] C. Song, T. Ono and M. Nomura, Bull. Chem. Soc. Jpn., 62 (1989) 630.
[8] C.M. Lee and C.N. Satterfield, Energy Fuel, 7 (1993) 978.
[9] M.J. Girgis and B.C. Gates, Ind. Eng. Chem. Res., 33 (1994) 1098.
[10] R.N. Landau, S.C. Korré, M. Neurock and M.T. Klein, in M.C. Oballa and S.S. Shih (Editors), Catalytic Hydroprocessing of Petroleum and Distillates, Marcel Dekker, New York, 1994, pp. 421–432.
[11] S.C. Korré, M.T. Klein and R.J. Quann, Ind. Eng. Chem. Res., 34 (1995) 101.
[12] D.C. Cronauer, D.M. Jewell, Y.T. Shah, R.J. Modi and K.S. Seshadri, Ind. Eng. Chem. Fundam., 18 (1979) 368.
[13] C. Song and K. Moffatt, Prepr. Am. Chem. Soc., Div. Petrol. Chem., 38 (1993) 779.
[14] C. Song and K. Moffatt, Microporous Mater., 2 (1994) 459.
[15] B.R. Cook and S.G. Colgrove, Prepr. Am. Chem. Soc., Div. Petrol. Chem., 39 (1994) 372.
[16] N.L. Allinger, F. Li, L. Yan and J.C. Tai, J. Comput. Chem., 11 (1990) 868.
[17] C. Song and S. Kirby, Microporous Mater., 2 (1994) 467.
[18] C. Song, H.H. Schobert and H. Matsui, Prepr. Am. Chem. Soc., Div. Fuel Chem., 36 (1991) 1892.
[19] A.D. Schmitz, G. Bowers and C. Song, Prepr. Am. Chem. Soc., Div. Fuel Chem., 40 (1995) 930.
[20] C. Song, W.-C. Lai and H.H. Schobert, Ind. Eng. Chem. Res., 33 (1994) 534.
[21] A.K. Ghosh and G. Curthoys, J. Phys. Chem., 88 (1984) 1130.
[22] J.-L. Lemberton and M. Guisnet, Appl. Catal., 13 (1984) 181.
[23] W.-C. Lai and C. Song, Prepr. Am. Chem. Soc., Div. Fuel Chem., 40 (1995) 1018.
[24] J.B. Pedley, R.D. Naylor and S.B. Kirby, Thermochemical Data of Organic Compounds, Chapman and Hall, London, 1986.